Lower crustal variability and the crust/mantle transition at the Atlantis Massif oceanic core complex

Donna K. Blackman[1] and John A. Collins[2]

Received 19 August 2010; revised 12 October 2010; accepted 19 October 2010; published 18 December 2010.

[1] Seismic refraction data provide new constraints on the structure of the lower oceanic crust and its variability across the Atlantis Massif oceanic core complex, ~30°N on the Mid-Atlantic Ridge. A 40 km-long spreading-parallel profile constrains P-wave velocities to depths of up to ~7 km beneath the seafloor. Two shorter spreading-perpendicular lines provide coverage to ~2 km depth. The anomalous character of the massif's central dome crust is clear compared to the neighboring rift valley and similar-age crust on the opposite ridge flank. The domal core of the massif, unroofed via detachment faulting, has velocities >7.0 km/s at depths below ~2.5 km sub-seafloor, increasing to 7.5–7.8 km/s over the depth range 4.8–6.8 km. Within the core complex, the Moho does not appear to be sharp as no PmP arrivals are observed. Within the axial valley, velocities do not reach mantle-transition zone values in the uppermost 6 km. We infer that crust there is of normal thickness but that a thinner than average mafic section is present in the central massif. Near IODP Hole U1309D, located on the central dome, there is a low velocity gradient interval at 1–3 km depth with velocities of 6.6–6.8 km/s, that coincides with a 3–5 km wide region where shallower velocities are highest. Given the predominantly gabbroic section recovered from the 1.4 km deep drillhole, this seismic structure suggests that the mafic body extends a few km both laterally and vertically. **Citation:** Blackman, D. K., and J. A. Collins (2010), Lower crustal variability and the crust/mantle transition at the Atlantis Massif oceanic core complex, *Geophys. Res. Lett.*, *37*, L24303, doi:10.1029/2010GL045165.

1. Introduction

[2] Recent recognition that detachment faulting and core-complex development play a notable role in the formation of slow-spread oceanic lithosphere [*Escartín et al.*, 2008; *Smith et al.*, 2006] provides a framework for our analysis of seismic refraction data that were collected in 1997 at Atlantis Massif, ~30°N on the Mid-Atlantic Ridge. The results of short-offset (2–6 km source-receiver range) refraction data have been reported previously [*Canales et al.*, 2008; *Collins et al.*, 2009; *Henig et al.*, 2009]. While shallow seismics and seafloor mapping provide important insights, they are not able to address some of the fundamental questions about oceanic core complex (OCC) structure that are key for testing models of their development. Here, we discuss the results of longer offset (15–40 km) ocean bottom seismograph (OBS) refraction experiments at Atlantis Massif that constrain structure and variability extending to depths of ~7 km sub-seafloor, much deeper than the ~1.5 km sub-seafloor region known from prior studies.

[3] Oceanic core complexes are hypothesized to form when detachment faulting persists for 1–2 Myr, and this localization of the plate boundary combines with ongoing extension (average half-rate 12 km/Myr in the study area [*Pariso et al.*, 1996]) to exhume plutonic rocks. If crustal production is largely complete at the time (place) that the detachment dominates [*Ildefonse et al.*, 2007; *Karson*, 1990], the expectation is that the crust/mantle boundary would be uplifted in concert with the exhumed domal core. If the detachment is active during magmatic accretion, as some models predict [*Dick et al.*, 2000; *Olive et al.*, 2010], then the distribution of mafic crustal intrusions within the ultramafic mantle host may be complex. The common detection of a Mohorovicic discontinuity (Moho) at 6–7 km depth [e.g., *White et al.*, 1992] in marine seismic studies indicates that the crust/mantle boundary is often a distinct interface (or at least a zone with thickness that is less than or of the order of a ~10 Hz seismic wavelength [*Spudich and Orcutt*, 1980]). The contrast in velocities across the discontinuity can be explained by (crustal) gabbro overlying (mantle) peridotite. However, velocities are also compatible with the lower (seismically-defined) crust being composed of peridotite partially altered by reaction with seawater infiltrating along fractures. By characterizing the 2–7 km deep seismic structure at Atlantis Massif, we aim to determine whether unaltered peridotite occurs in the vicinity of the OCC and to assess the nature of the crust/mantle transition. In addition, documentation of the lateral variability in seismic structure can inform models of the extent of possible magmatic intrusion during OCC development and/or the degree of alteration of mantle rock that resides at depths shallower than the classic layered ocean crust model predicts.

[4] Results of OBS refraction studies are available for a few other OCCs in the Indian Ocean, Philippine Sea, and south Atlantic [*Muller et al.*, 2000, *Minshull et al.*, 2006; *Ohara et al.*, 2007; *Planert et al.*, 2010]. However, the combination of seafloor mapping, deep drilling, and close-spaced OBSs with a large airgun array is unique to Atlantis Massif.

[5] Seismic data were acquired with the R/V Maurice Ewing in 1997, a year after the Atlantis Massif had been recognized as an oceanic core complex [*Cann et al.*, 1997]. In addition to the traditional seafloor-receiver/surface-source refraction Lines 8, 9a and 9b, emphasized here (Figure 1), two short seafloor-receiver/seafloor-source refraction lines were acquired in the middle of Lines 9a and 9b on the Central Dome of the massif. In 2001, the Ewing

[1]Scripps Institution of Oceanography, University of California, San Diego, La Jolla, California, USA.
[2]Woods Hole Oceanographic Institution, Woods Hole, Massachusetts, USA.

0094-8276/10/2010GL045165

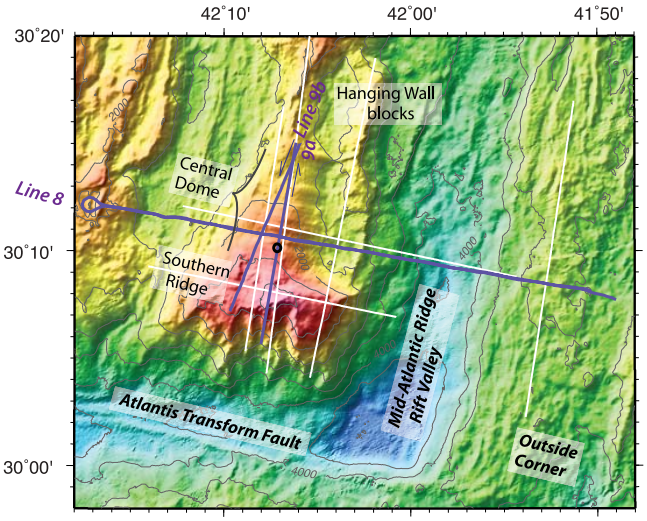

Figure 1. Map of Atlantis Massif, MAR 30°N region showing the locations of the OBS refraction (purple) and MCS reflection (white) lines discussed in the text. Corrugated dome marks the exposed detachment underlain by mafic ± ultramafic plutonic "core complex". Black circle marks the location of IODP Hole U1309D.

returned to the area for a multi-channel seismic (MCS) survey [*Canales et al.*, 2004], for which lines Meg10 and Meg4 approximately coincide with refraction Lines 8 and 9a, respectively (Figure 1). Streamer refraction analyses (up to 6 km source receiver offset; [*Canales et al.*, 2008; *Henig et al.*, 2009]) and the 2-km offset, on-bottom refraction results [*Collins et al.*, 2009] constrain seismic structure in the upper ~1 km only. With the traditional OBS refraction data analyzed here, we can address the structure of the lower crust and constrain the existence and nature of the Moho across this OCC.

2. Data Acquisition and Analyses

[6] The OBSs were deployed at 5–9 km spacing (Figure 2 and Figures S1 and S4 of the auxiliary material), and instrument locations on the seafloor were determined by inverting travel-times of the direct water-wave arrival from nearby shots (Table S1 of the auxiliary material).[1] A minimum-phase filter was applied to the data, with pass bands of 5–20 Hz (Line 8) or 5–30 Hz (Line 9a and 9b). The high-relief seafloor topography has a significant influence on the pattern of the refracted arrivals (Figure 2), making it difficult to discern even general subsurface structure from visual inspection of the record sections.

[7] The times of the first-arriving refractions were picked on individual traces and checked in the full record section. Pick times were fine-tuned using cross-correlation when nearby arrivals shared a common waveform. Pick uncertainties ranged from 15–40 ms, with 20–25 ms being typical. Sample rates for the OBSs varied from 0.833 to 5.0 ms.

[8] We employed the tomographic method reported by van Avendonk [*Van Avendonk et al.*, 2004]. Initial starting models consisted of an average 1-D profile, with somewhat higher than typical velocities and gradients in the upper ~1.5 km [*Canales et al.*, 2008], draped from the seafloor along each line. For Line 8, a series of other starting models were also employed in order to test the robustness of the main structure in the tomographic result. In addition to changing the average velocity-depth profile of some Line 8 starting models, we also included shallow variability determined from the streamer refraction study by *Canales et al.* [2008]. Model damping values were reduced over a series of inversions, each with target χ^2 adjusted closer to 1 than the prior run. The overall χ^2 for the tomographic models is 0.9–1; reducing χ^2 slightly below 1 for the overall fit ensures that the travel-times for each individual gather also have $\chi^2 \sim 1$.

3. OBS Refraction Models

[9] Lateral variability in lithospheric structure across the OCC at depths of 1.5 to ~7 km follows the basic distribution recognized in prior shallow seismic studies. Velocities are high beneath the eastern slope of the Central Dome, and the spreading axis has a velocity structure that is typical for young Atlantic crust (Figure 2). Beneath the western slope of the dome, velocities in the upper kilometer are normal (increasing in the range 3.5 to 5.2 km/s) whereas the eastern slope is characterized by velocities that exceed 5 km/s at depths greater than 200 mbsf. Throughout the dome, values of 7 km/s are reached at depths that are more than a km shallower than normal (~2.5 km instead of 3.7–4.7 km [*White et al.*, 1992]). The outside-corner crust falls within the typical Atlantic velocity envelope but is slower than axial crust by ~0.5 km/s at depths of 2.5–3 km.

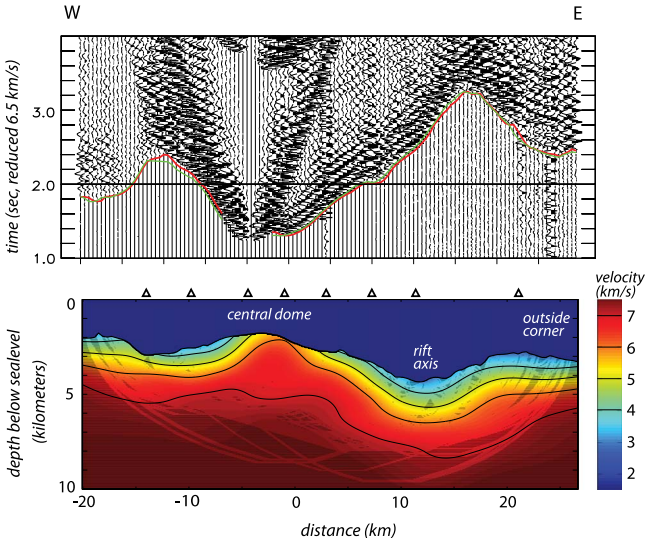

Figure 2. Representative record section and P-wave tomographic model for Line 8. OBS locations are shown by triangles; section shown is for third instrument from west. Travel-time picks are traced by red line; predicted first-arrival times for this model are traced in green. Dark-shaded area indicates no ray coverage for the model. Data require higher than average velocity within the domal core above 5 km depth (starting models with normal velocity-depth profile were tested, as well as the higher than average, shallow gradient starting model used in this inversion). Deeper velocity values >7.5 km/s are also robust.

[1] Auxiliary materials are available in the HTML. doi:10.1029/2010GL045165.

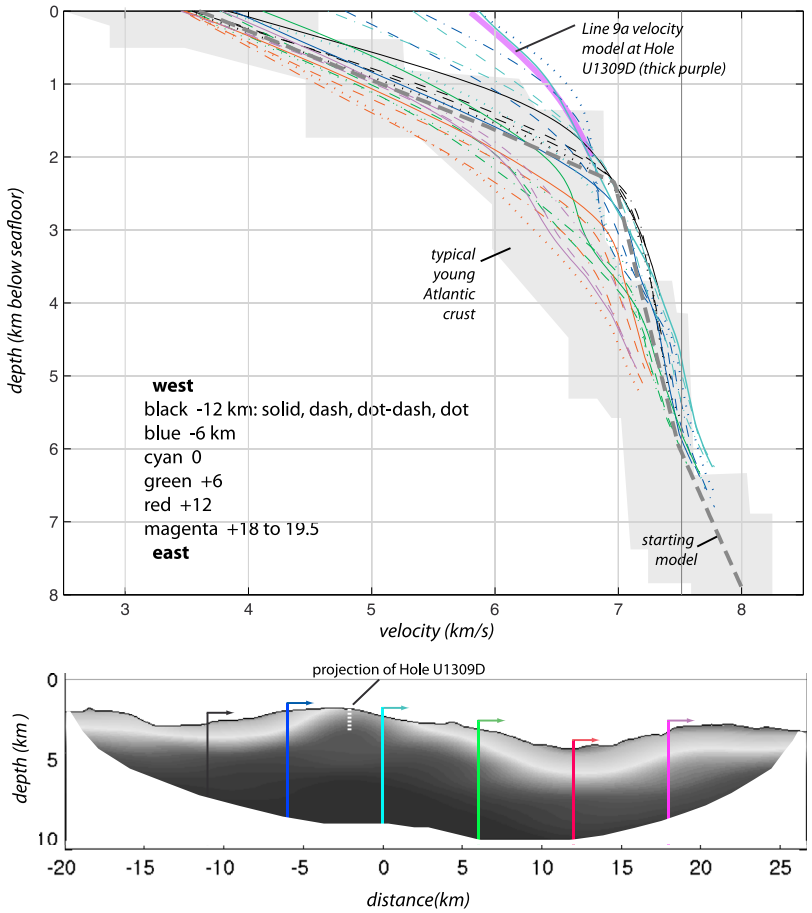

Figure 3. Velocity-depth profiles along Line 8, spaced 1.5 km in portion of model where coverage is good. Intervals of 6-km length are color-coded, and line type varies west–east from solid to dash, dot-dash, and dotted, within each interval. Preferred velocity model (grayshade version of Figure 2 with no vertical exaggeration) is shown below with color intervals marked at each western edge. Shaded area on upper plot marks the velocity-depth envelope of young Atlantic crust [*White et al.*, 1992].

[10] The Line 9a and 9b results are consistent with the prior MCS refraction results [*Canales et al.*, 2008] showing that the Central Dome has velocities that are faster than the Southern Ridge (Figure S4). The difference in velocity decreases from 1.5 km/s just below the seafloor to ~0.5 km/s at the base of our coverage around 2.5 km depth. Velocities in the upper ~1.5 km along Line 9b are consistently 0.2–0.5 km/s lower than those determined at similar along-strike position in Line 9a, which is to the east (Figure S4).

[11] Only beneath the Central Dome are velocities of 7.5–7.8 km/s required at depths less than 6 km (Figure 2). The tomographic results for a suite of starting models with various Moho depths and sharpness (Figures S3 and S5), together with the lack of clear PmP or 'breakout' Pn arrivals (Figures 2 and S2) indicate that the crust/mantle transition is not sharp beneath the OCC. We determine a fairly constant increase from 7 to 7.8 km/s within most of the domal core, although beneath the apex (−3 km in the model) and under the adjacent hanging wall block (+4.5–6 km) a constant-velocity interval of ~6.8 km/s at 2–3 km subseafloor is found (Figure 3). The data do not allow models where the Moho within the OCC is less than ~4 km deep but all results (including models for 6-km deep starting Moho depth) indicate that the base of the crust/mantle transition shoals to between 4.5 and 5 km depth beneath the domal core, more noticeably in the east (−3 to +3 km, Figure 3).

[12] The main features of the tomographic model in Figure 2 are robust, in particular the deeper structure that we focus on here. Differences in velocity models that fit the data well ($\chi^2 \sim 1$) using different starting models are generally less than 0.1 km/s within the OCC, where coverage by crossing raypaths is good (Figure S5).

4. Discussion

[13] The travel-time data rule out the occurrence of significant amounts of unaltered ultramafic rock in the upper ~4.5 km of the detachment footwall within the Central Dome. While short-offset, on-bottom refraction [*Collins et al.*, 2003] and MCS reflection patterns within the OCC [*Canales et al.*, 2004] were initially interpreted to indicate a crust/mantle boundary at depths of less than 1 km, all subsequent studies have shown that the crust/mantle boundary in the Central Dome must be deeper [*Blackman et al.*, 2008; *Canales et al.*, 2008; *Collins et al.*, 2009]. Our finding of velocities that surpass 7.5 km/s at 4.5–5.5 km depths under the eastern slope of the dome indicates that the crust/mantle transition is shallower than average in portions of the OCC. Under the western slope of the dome, mantle-like velocities

are reached at ~6 km depth with values in the 7.5–7.8 km/s range. Our coverage does not allow determination of Moho character or depth outside the OCC, although we can confirm that it is not shallower than average beneath the current spreading axis. Gravity modeling supports an interpretation that the crust/mantle boundary shoals to ~4.5 km subseafloor within the footwall to the detachment, but is of more typical depth (6–7 km) in adjacent older and younger lithosphere [*Blackman et al.*, 2008].

[14] We recognize 3 general velocity-depth patterns. 1) The axial valley, rift walls, and outside-corner have a normal velocity-depth structure. The youngest crust in the center of the rift valley has higher velocities in the 2–3 km depth range than the rift walls or outside -corner and this likely reflects increased porosity in the latter due to fracturing associated with faulting as the rift mountains form. 2) Much of the core complex shows a steady increase in velocity to ~7 km/s at about 2.5 km depth; this interval is underlain by material with a lower gradient that is characterized by velocities of 7.8 km/s at 6–7 km depth. The velocity near the seafloor varies across the dome, from normal values in the west to values of 5.3 to 5.8 km/s over the apex of the dome and then dropping below 5 km/s where the hanging wall blocks overly the footwall. 3) Beneath the eastern slope of the dome and underneath the immediately adjacent hanging wall block there is a low velocity gradient interval at 1 to ~3 km depth with velocities of 6.6–6.8 km/s. Together, the velocities and gradient are suggestive of classic upper layer 3 seismic structure [*Spudich and Orcutt*, 1980] and this region of low gradient is found just 1.1 km from IODP Hole U1309D. Line 9a crosses directly over the drill site and the velocity profile to 2 km depth (the limit of coverage) overlaps the Line 8 profiles near that area (Figure 3). The recovery of a dominantly gabbroic section from the 1.4 km deep drill hole [*Blackman et al.*, 2006], and the occurrence of shallow high velocities underlain by classic layer 3 low-gradient, 6.5–6.8 km/s velocities in our tomographic model, suggest that this body of mafic intrusives extends at least 3 km both laterally and vertically. The E–W lateral extent of the low-gradient interval is less than 5 km. This potential constraint on the extent of the gabbroic body sampled by drilling warrants further investigation. We know that some of the shallow (<300 m) structure that the MCS data require has been smoothed out by our inversion (compare the starting model in Figure S5 (top) with inversion results, Figures 2 and S5 (middle)). None-the-less, the area where we discern the low-gradient interval is covered by many crossing rays and the derivative weight sums show significant influence of tomographic model elements throughout this area, so the basic structure will remain unchanged, while detailed velocity values may shift somewhat if MCS refraction picks are directly incorporated in the inversion.

[15] Peridotite likely is present within the central domal core. With the exception of the low-gradient body just discussed, the footwall velocities of 7.2–7.6 km/s determined below ~2.5 km depth are consistent with olivine-rich rock that is altered less than ~20% [e.g., *Horen et al.*, 1996]. Olivine-rich (troctolite, dunite, and wehrlite) lenses are known to occur within oceanic core complexes [*Blackman et al.*, 2006; *Dick et al.*, 2008; *Kelemen et al.*, 2007; *Natland and Dick*, 2002] and within the crust/mantle transition zone of many ophiolites [*Karson et al.*, 1984; *Collins et al.*, 1986; *Boudier and Nicolas*, 1995]. Given that the thickness of such lenses mapped at OCCs to date is an order of magnitude smaller than the few-km thick interval required by our data, our observations may be better explained by mantle peridotite either intruded by small mafic bodies and/or altered by seawater circulation to decreasing extent with depth [*Minshull et al.*, 1998].

[16] A simple geological model where the western flank of the central dome is a flexurally uplifted classic oceanic crustal section offset along a detachment fault does not appear to fit our results. While velocities of the upper few hundred meters at horizontal distances −11 to −6 km (Figure 3) are typical for oceanic crust (consistent with expected values for porous basalt), the vertical velocity gradients in this region are anomalously high, with velocities in excess of 6.5 km/s observed at sub-seafloor depth of 2 km. The velocity profiles for this region are resolvably different from those measured beneath the axial valley or outside-corner.

[17] The Line 9a and 9b results show that the western parts of both the central and southern domes have velocities that are ~0.5 km/s slower in the upper 1.5 km than the eastern parts. Greater alteration in the longer-exposed western portion of a constant lithology core is a simple explanation. However, primary rock type may also play a role if the eastern portion of the dome is dominantly gabbroic, and seafloor to the west consists of a fractured basaltic carapace [*Blackman et al.*, 2008]. Alternatively, the western flank could be dominantly peridotite, with fewer mafic intrusions than occur in the dominantly gabbroic eastern flank, and serpentinization could be responsible for the lower velocities determined there. The latter scenario follows that proposed to explain along-strike variability at Atlantis Massif [e.g., *Karson et al.*, 2006] and across-strike variability at the Kane OCC [*Xu et al.*, 2009].

[18] **Acknowledgments.** NSF grants provided support for the data acquisition, initial interpretation (Collins OCE-9633114 and OCE-9819297) and subsequent processing and analysis (Blackman OCE-0927442). IODP Expeditions 304/305 provided groundtruth at Site U1309. Alistair Harding provided code and guidance at some stages of the analysis.

References

Blackman, D. K., et al. (2006), *Oceanic Core Complex Formation, Atlantis Massif*, *Proc. Integr. Ocean Drill. Program*, *304/305*.

Blackman, D. K., G. D. Karner, and R. C. Searle (2008), Three-dimensional structure of oceanic core complexes: Effects on gravity signature and ridge flank morphology, Mid-Atlantic Ridge 30°N, *Geochem. Geophys. Geosyst.*, *9*, Q06007, doi:10.1029/2008GC001951.

Boudier, F., and A. Nicolas (1995), Nature of the Moho transition zone in the Oman ophiolite, *J. Petrol.*, *36*, 777–796.

Canales, J. P., et al. (2004), Seismic reflection imaging of an oceanic detachment fault: Atlantis megamullion (Mid-Atlantic Ridge, 30°10′N), *Earth Planet. Sci. Lett.*, *222*, 543–560, doi:10.1016/j.epsl.2004.02.023.

Canales, J. P., B. E. Tucholke, M. Xu, J. A. Collins, and D. L. DuBois (2008), Seismic evidence for large-scale compositional heterogeneity of oceanic core complexes, *Geochem. Geophys. Geosyst.*, *9*, Q08002, doi:10.1029/2008GC002009.

Cann, J. R., et al. (1997), Corrugated slip surfaces formed at ridge-transform intersections on the Mid-Atlantic Ridge, *Nature*, *385*, 329–332, doi:10.1038/385329a0.

Collins, J. A., T. M. Brocher, and J. A. Karson (1986), Two-dimensional seismic reflection modeling of the inferred fossil oceanic crust/mantle transition in the Bay of Islands ophiolite, *J. Geophys. Res.*, *91*, 12,520–12,538, doi:10.1029/JB091iB12p12520.

Collins, J., et al. (2003), Seismic velocity structure of mid-Atlantic ridge core complexes, *Geophys. Res. Abstr.*, Abstract EAE03-A-10390.

Collins, J. A., D. K. Blackman, A. Harris, and R. L. Carlson (2009), Seismic and drilling constraints on velocity structure and reflectivity near IODP Hole U1309D on the central dome of Atlantis Massif,

Mid-Atlantic Ridge 30°N, *Geochem. Geophys. Geosyst.*, *10*, Q01010, doi:10.1029/2008GC002121.

Dick, H. J. B., et al. (2000), A long in situ section of lower ocean crust: Results of ODP Leg 176 drilling at the southwest Indian Ridge, *Earth Planet. Sci. Lett.*, *179*, 31–51, doi:10.1016/S0012-821X(00)00102-3.

Dick, H. J. B., M. A. Tivey, and B. E. Tucholke (2008), Plutonic foundation of a slow-spreading ridge segment: the oceanic core complex at Kane Megamullion, 23°30′N, 45°20′W, *Geochem. Geophys. Geosyst.*, *9*, Q05014, doi:10.1029/2007GC001645.

Escartín, J., et al. (2008), Central role of detachment faults in accretion of slow-spreading oceanic lithosphere, *Nature*, *455*, 790–794, doi:10.1038/nature07333.

Henig, A. S., et al. (2009), Seismic velocity variation within the footwall of an oceanic core complex–Atlantis Massif, Mid-Atlantic Ridge 30°N, *InterRidge Newsl.*, *18*, 9–13.

Horen, H., M. Zamora, and G. Dubuisson (1996), Seismic wave velocities and anisotropy in serpentinized peridotites from Xigaze ophiolite: Abundance of serpentinite in slow spreading ridge, *Geophys. Res. Lett.*, *23*, 9–12, doi:10.1029/95GL03594.

Ildefonse, B., et al. (2007), Oceanic core complexes and crustal accretion at slow-spreading ridges, *Geology*, *35*(7), 623–626, doi:10.1130/G23531A.1.

Karson, J. A. (1990), Seafloor spreading on the Mid-Atlantic Ridge: implications for the structure of ophiolites and oceanic lithosphere produced in slow-spreading environments, in *Proceedings of Symposium Troodos 1987*, edited by J. Malpas, pp. 547–553, Geol. Surv. Dep., Nicosia.

Karson, J. A., J. A. Collins, and J. F. Casey (1984), Geologic and seismic velocity structure of the crust/mantle transition in the Bay of Islands ophiolite complex, *J. Geophys. Res.*, *89*, 6126–6138, doi:10.1029/JB089iB07p06126.

Karson, J. A., G. L. Früh-Green, D. S. Kelley, E. A. Williams, D. R. Yoerger, and M. Jakuba (2006), Detachment shear zone of the Atlantis Massif core complex, Mid-Atlantic Ridge, 30°N, *Geochem. Geophys. Geosyst.*, *7*, Q06016, doi:10.1029/2005GC001109.

Kelemen, P. B., et al. (2007), *Proceedings of the Ocean Drilling Program, Scientific Results*, 209, doi:10.2973/odp.proc.sr.209.2007.

Minshull, T. A., et al. (1998), Is the oceanic Moho a serpentinization front? in *Modern Ocean Floor Processes and the Geological Record*, edited by R. A. Mills and K. Harrison, pp. 71–80, Geol. Soc., London.

Minshull, T. A., et al. (2006), Crustal structure of the Southwest Indian Ridge at 66°E: seismic constraints, *Geophys. J. Int.*, *166*, 135–147, doi:10.1111/j.1365-246X.2006.03001.x.

Muller, M. R., et al. (2000), Crustal structure of the Southwest Indian Ridge at the Atlantis II Fracture Zone, *J. Geophys. Res.*, *105*(B11), 25,809–25,828, doi:10.1029/2000JB900262.

Natland, J., and H. J. B. Dick (2002), *Proceedings Ocean Drilling Program, Scientific Results*, 176, doi:10.2973/odp.proc.sr.176.2002.

Ohara, Y., et al. (2007), Seismic study on oceanic core complexes in the Parece Vela back-arc basin, *Isl. Arc*, *16*, 348–360, doi:10.1111/j.1440-1738.2007.00591.x.

Olive, J.-A., et al. (2010), The structure of oceanic core complexes controlled by the depth distribution of magma emplacement, *Nat. Geosci.*, *3*, 491–495, doi:10.1038/ngeo888.

Pariso, J. E., et al. (1996), Three-dimensional inversion of marine magnetic anomalies: implications for crustal accretion along the Mid-Atlantic Ridge (28°–31°30′N), *Mar. Geophys. Res.*, *18*, 85–101, doi:10.1007/BF00286204.

Planert, L., et al. (2010), Crustal structure of a rifted oceanic core complex and its conjugate side at the MAR at 5°S: Implications for melt extraction during detachment faulting and core complex formation, *Geophys. J. Int.*, *181*, 113–126, doi:10.1111/j.1365-246X.2010.04504.x.

Smith, D. K., et al. (2006), Widespread active detachment faulting and core complex formation near 13 degrees N on the Mid-Atlantic Ridge, *Nature*, *442*, 440–443, doi:10.1038/nature04950.

Spudich, P., and J. Orcutt (1980), A new look at the seismic velocity structure of the oceanic crust, *Rev. Geophys.*, *18*, 627–645, doi:10.1029/RG018i003p00627.

Van Avendonk, H. J. A., D. J. Shillington, W. S. Holbrook, and M. J. Hornbach (2004), Inferring crustal structure in the Aleutian arc from a sparse wide-angle seismic data set, *Geochem. Geophys. Geosyst.*, *5*, Q08008, doi:10.1029/2003GC000664.

White, R. S., D. McKenzie, and R. K. O'Nions (1992), Oceanic crustal thickness from seismic measurements and rare earth element inversions, *J. Geophys. Res.*, *97*, 19,683–19,715, doi:10.1029/92JB01749.

Xu, M., J. P. Canales, B. E. Tucholke, and D. L. DuBois (2009), Heterogeneous seismic velocity structure of the upper lithosphere at Kane oceanic core complex, Mid-Atlantic Ridge, *Geochem. Geophys. Geosyst.*, *10*, Q10001, doi:10.1029/2009GC002586.

D. K. Blackman, Scripps Institution of Oceanography, University of California, San Diego, 9500 Gilman Dr., La Jolla, CA 92093, USA. (dblackman@ucsd.edu)

J. A. Collins, Woods Hole Oceanographic Institution, Clark South 272, Woods Hole, MA 02543, USA.